Available online at www.sciencedirect.com

SCIENCE DIRECT®

Journal of Sound and Vibration 294 (2006) 1039–1050

JOURNAL OF SOUND AND VIBRATION

www.elsevier.com/locate/jsvi

Statistical characteristics of frequency response localization in nearly periodic systems

Sang Ha Shin[a], Se Jeong Lee[b], Hong Hee Yoo[a,*]

[a]*School of Mechanical Engineering, Hanyang University, 17 Haengdang-Dong Sungdong-Gu, Seoul 133-791, Korea*
[b]*School of Mechanical Engineering, University of Seoul, 90 Cheonnong-Dong Dongdaemun-Gu, Seoul 130-743, Korea*

Received 18 March 2005; received in revised form 14 November 2005; accepted 7 January 2006
Available online 28 February 2006

Abstract

Premature failures or malfunctions often occur in a mechanical system that has periodically repeated subcomponents. Due to slight irregularities among subcomponents of the periodic system, maximal frequency responses of a few subcomponents become often significantly larger than those of other subcomponents. These phenomena, called frequency response localization, need to be analyzed elaborately for reliable designs of the periodic systems. In the present study, the strength of frequency response localization for the periodic system is defined and the effects of some parameters on the strength of frequency response localization are investigated statistically.

1. Introduction

Periodic systems, in which several subcomponents are repeated, can be found in some engineering examples such as helicopter blades (the number of subcomponents is usually 2–4) and turbine blades (the number of subcomponents is usually more than 20). In periodic systems, however, their subcomponents are not perfectly identical since irregularities among subcomponents always exist due to manufacturing tolerances, material degeneration and operation wears. Such periodic systems that have slight irregularities among their subcomponents are called nearly periodic systems in this study. If all the subcomponents are perfectly identical and excited by an identical force, the magnitudes of their frequency responses should be identical, too. Compared to the identical frequency response (of a perfectly periodic system), those of a few subcomponents of a nearly periodic system often become significantly large. These phenomena, called the frequency response localization in this study, often cause unexpected premature failures of the periodic systems. Therefore, they should be analyzed elaborately for reliable designs of the systems.

Since Anderson [1] pioneered the localization phenomena in solid-state physics, the localization phenomena have drawn attention from several researchers in engineering fields. Ewins [2–5] showed that the maximal forced response increases with increasing irregularity among subcomponents of a periodic system up to certain level. However, further increase results in lower forced response. Bendiksen [6,7] investigated the mode

*Corresponding author. Tel.: +82 2 2220 0446; fax: +82 2 2293 0570.
E-mail addresses: shshin@ihanyang.ac.kr (S.H. Shin), selee@uos.ac.kr (S.J. Lee), hhyoo@hanyang.ac.kr (H.H. Yoo).

0022-460X/$ - see front matter
doi:10.1016/j.jsv.2006.01.002

localization of the turbine blade system using a simple coupled pendulum system. Pierre et al. [8,9] investigated the mode localization of a multi-span system by perturbation method and also introduced intentional irregularities [10,11] into the design of a bladed-disk system to reduce maximal transient responses.

When a subcomponent of a periodic system is excited, the transient response decays away from the excitation source. The rate of decay is normally quantified by a parameter known as localization factor, which has been often used to measure the strength of the localization. The localization factor due to irregularity was first defined by Hodges and Woodhouse [12], and employed to investigate localization phenomena in periodic systems by several other researchers (see, for instance, Refs. [13–15]). More recently, Yoo et al. [16] introduced a different way of analyzing localization, which employs multi-excitation forces acting on all subcomponents of a periodic system simultaneously. By employing the multi-excitation force model, they found that strong frequency response localization could occur when the pendulum length irregularity was related to the coupling stiffness in a specific way.

Several analytical methods were also developed to obtain statistical results for nearly periodic systems. Huang [17] considered the blade lengths as statistical variables and developed an analytical method to generate the mean and the variance of the blade vibration amplitudes, which employs a perturbation technique. Sinha [18] combined the first-order perturbation method with a statistical theory to yield probability density functions. Wei and Pierre [19] showed that some statistical properties such as the mean and the variance of the largest amplitude cannot be generated through the aforementioned analytical techniques. They showed that the Monte Carlo simulation method could be applied to obtain the statistical properties for weakly coupled systems.

In the present study, the multi-excitation force model introduced in Ref. [16] is employed to investigate the frequency response localization phenomena. A simple definition of the strength of frequency response localization is proposed and the effects of some parameters on the localization strength are investigated statistically by employing a coupled multi-pendulum model. The probabilities (that the localization strength exceeds a certain value) versus the statistical properties of the parameters are calculated through Monte Carlo simulation. The present approach is especially valuable for the designs of periodic systems to avoid (or enhance) the frequency response localization.

2. Simplified modeling of nearly periodic systems

Nearly periodic systems consist of repeated subcomponents that possess nearly identical structural topology. Fig. 1 shows a coupled pendulum system that represents the nearly periodic system. Each pendulum, which is a subcomponent of the nearly periodic system, consists of a mass m, a rotational spring having

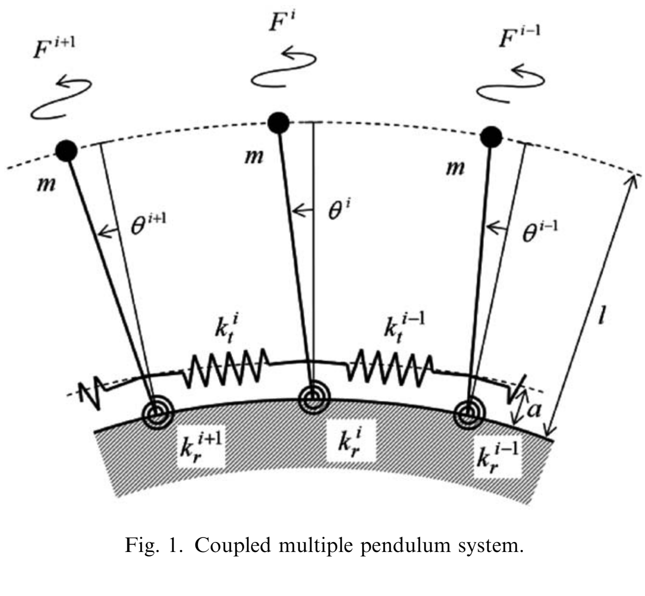

Fig. 1. Coupled multiple pendulum system.

modulus k_r^i, and two translational springs having modulus k_t^i and k_t^{i-1}. The distances from a hinge point to a translational spring attachment point and the length of all pendulums are denoted by a and l, respectively. Even though damping is not shown in Fig. 1, linear viscous damping force is assumed to act on every pendulum mass. The damping constant and the excitation force for the ith pendulum are denoted by c^i and F^i, respectively. Then the equation of motion of the ith pendulum can be derived as follows:

$$ml^2\ddot{\theta}^i + c^i l^2\dot{\theta}^i + k_r^i\theta^i - k_t^{i-1}a^2\theta^{i-1} + (k_t^{i-1} + k_t^i)a^2\theta^i - k_t^i a^2\theta^{i+1} = F^i l. \tag{1}$$

To obtain more general and useful conclusions, the equations of motion are transformed into dimensionless forms. For the purpose, three dimensionless parameters and two dimensionless variables are defined as follows:

$$\zeta_i \equiv \frac{c^i l}{2\sqrt{mk_r^i}}, \quad \omega_i = \sqrt{\frac{k_r^i/ml^2}{k_r/ml^2}}, \quad \beta_i \equiv \frac{a^2k_t^i}{k_r}, \quad f_i \equiv \frac{F^i l}{k_r^i}, \quad \tau \equiv \sqrt{\frac{k_r}{ml^2}}t, \tag{2}$$

where k_r represents the mean of k_r^i's. The physical meanings of ς_i, β_i, f_i and τ are damping ratio, dimensionless coupling stiffness, dimensionless excitation force, and dimensionless time, respectively. The symbol ω_i denotes the dimensionless natural frequency of the ith pendulum when the pendulum has no coupling stiffness.

Since the variation of the dimensionless natural frequency ω_i can be achieved by changing the rotational spring stiffness (k_r^i), the mass and the length of all pendulums are assumed constant in this study. Also, the distance a is assumed constant since the variation of the dimensionless coupling stiffness β_i can be achieved by changing the translational spring stiffness (k_t^i).

Employing the three dimensionless parameters and variables, Eq. (1) can be rewritten as follows:

$$\ddot{\theta}^i + 2\zeta_i\omega_i\dot{\theta}^i + \omega_i^2\theta^i + (\beta_{i-1} + \beta_i)\theta^i - \beta_{i-1}\theta^{i-1} - \beta_i\theta^{i+1} = \omega_i^2 f_i, \tag{3}$$

where a dot over a symbol now represents the differentiation of the symbol with respect to the dimensionless time τ. Therefore, the equations of motion of the pendulum system can be written in a matrix form as follows:

$$\{\ddot{\theta}\} + [C]\{\dot{\theta}\} + [K]\{\theta\} = \{f\}, \tag{4}$$

where

$$[C] = \begin{bmatrix} 2\zeta_1\omega_1 & 0 & \cdots & \cdots & 0 \\ 0 & \ddots & \ddots & \ddots & \vdots \\ \vdots & \ddots & 2\zeta_i\omega_i & \ddots & \vdots \\ \vdots & \ddots & \ddots & \ddots & 0 \\ 0 & \cdots & \cdots & 0 & 2\zeta_n\omega_n \end{bmatrix}, \quad \{f\} = \begin{Bmatrix} f_1 \\ \vdots \\ f_i \\ \vdots \\ f_n \end{Bmatrix},$$

$$[K] = \begin{bmatrix} \omega_1^2 + (\beta_n + \beta_1) & -\beta_1 & 0 & 0 & -\beta_n \\ -\beta_1 & \ddots & \ddots & 0 & 0 \\ 0 & -\beta_{i-1} & \omega_i^2 + (\beta_{i-1} + \beta_i) & -\beta_i & 0 \\ 0 & 0 & \ddots & \ddots & -\beta_{n-1} \\ -\beta_n & 0 & 0 & -\beta_{n-1} & \omega_n^2 + (\beta_{n-1} + \beta_n) \end{bmatrix}. \tag{5}$$

Taking Fourier transformation of Eq. (4) yields the following matrix equation:

$$(-\omega^2[I] + j\omega[C] + [K])\{\bar{\theta}\} = \{\bar{f}\}, \tag{6}$$

where $\{\bar{\theta}\}$ and $\{\bar{f}\}$ are the Fourier transformations of $\{\theta\}$ and $\{f\}$, respectively. Now, from Eq. (6), one can obtain $\{\bar{\theta}\}$ which represents the frequency response of the pendulum system. The frequency response amplitude of the ith pendulum is $|\bar{\theta}_i|$. Substituting $\bar{\theta}_i = X_i + jY_i$ into Eq. (6), the following equation can be derived:

$$\begin{bmatrix} -\omega^2[I]+[K] & -\omega[C] \\ \omega[C] & -\omega^2[I]+[K] \end{bmatrix} \begin{Bmatrix} \{X\} \\ \{Y\} \end{Bmatrix} = \begin{Bmatrix} \{\bar{f}\} \\ 0 \end{Bmatrix}. \tag{7}$$

The excitation forces, acting on all pendulums, are assumed to have the same white random property in the present study. So, a constant value for $\bar{f}_i$ is used to obtain X_i and Y_i. However, any pattern of $\bar{f}_i$ may be employed for the analysis if needed.

Since $|\bar{\theta}_i|$ is a function of ω, the maximum value of $|\bar{\theta}_i|$, denoted as $|\bar{\theta}_{i\ \max}|$, exists at a certain frequency ω. The frequency (at which the maximum frequency response occurs) can be obtained by solving an eigenvalue problem for which the mass, the damping, and the stiffness matrices in Eq. (4) are employed.

The strength of frequency response localization will be defined by comparing the maximum frequency responses ($|\bar{\theta}_{i\ \max}|$'s) of a nearly periodic system to a standard value $|\bar{\theta}_{\mathrm{st}}|$. For the reference value $|\bar{\theta}_{\mathrm{st}}|$, the maximum frequency response of an uncoupled perfectly periodic system (i.e. $\omega_i = 1$, $\beta_i = 0$) with a standard damping ratio ς_{st} will be employed. Now, dimensionless maximum frequency responses of a nearly periodic system are defined as follows:

$$\kappa_i \equiv \frac{|\bar{\theta}_{i\ \max}|}{|\bar{\theta}_{\mathrm{st}}|}. \tag{8}$$

Then the strength of frequency response localization is defined as the maximum value among κ_i's and it will be denoted as κ. Thus,

$$\kappa = \mathrm{Max}(\kappa_1, \kappa_2, \ldots, \kappa_n). \tag{9}$$

Since κ_i depends on the value of the standard damping ratio ς_{st}, κ also depends on the value, too. Later, a small value for ς_{st} will be chosen for the numerical simulation since the lightly damped periodic system is the major concern in this study.

3. Numerical results and discussion

In the present section, the probability that the frequency response localization strength exceeds certain value will be calculated through Monte Carlo simulation for which ω_i, β_i, and ς_i are employed as input parameters. Normal distributions for the input parameters are assumed in the present study even if the distribution patterns of actual problems may differ from the normal distribution. The effects of various distribution patterns on the frequency response localization phenomena are not considered in the present study.

The simulation procedure can be summarized as follows. Input parameter sets are created with a random number generator. The number of parameter sets that is enough to guarantee the convergence of the statistical properties of the output (the frequency response localization strength) is determined first through convergence study. Then, for each parameter set, the frequency response equations are solved and the strength of the localization is calculated. Lastly, by counting the number of samples in which a given criterion for the localization strength is satisfied, the probability is calculated.

The following simple case is considered first to explain the frequency response localization. The number of pendulum is 2 and all the system parameters are given as deterministic values. As the index number changes, ω_i may vary while ς_i and β_i remain invariant. In other words, $\varsigma_1 = \varsigma_2 = \varsigma$ and $\beta_1 = \beta_2 = \beta$. The following three sets (for ω_1, ω_2, ς, β) are employed to obtain frequency responses: (1.0, 1.0, 0.005, 0.002), (1.0, 1.024, 0.005, 0.002), and (1.0, 1.024, 0.005, 0.012). Numerical results for the three sets are shown in Fig. 2. Fig. 2(a) shows the frequency response curves of the first set. Since no irregularity exists in this case, the frequency response curves for the two pendulums are identical. Figs. 2(b) and (c) show the frequency response curves of the second and the third sets. As shown in the figures, the small irregularity between ω_1 and ω_2 causes the significant difference of frequency response curves. It can also be observed that the coupling stiffness variation (see the difference between Figs. 2(b) and (c)) could increase the frequency response difference more significantly.

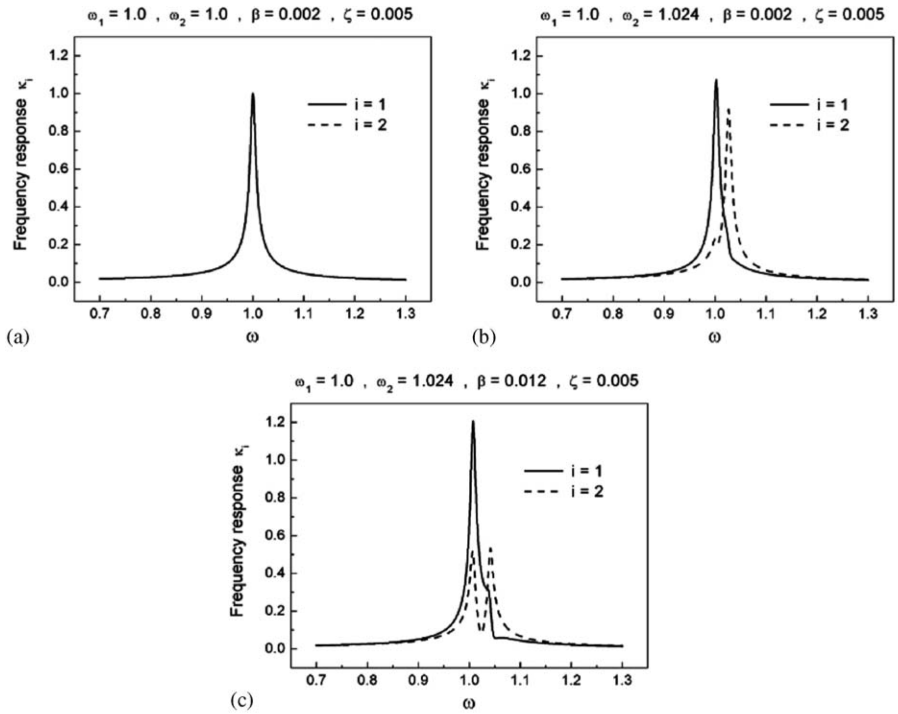

Fig. 2. Frequency response curves obtained with three parameter sets. (a) Identical curves for same natural frequencies, (b) distinct curves for different natural frequencies (with the weaker coupling stiffness), and (c) distinct curves for different natural frequencies (with the stronger coupling stiffness).

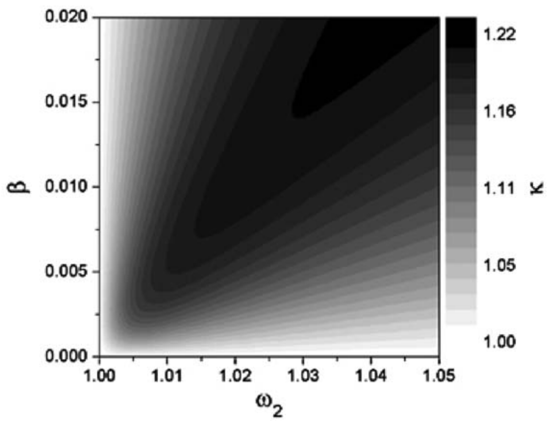

Fig. 3. The strength of frequency response localization in ω_2–β plane ($\omega_1 = 1.0$, $\varsigma = 0.005$).

Fig. 3 shows the variation of the localization strength κ in ω_2–β plane, where $\omega_1 = 1.0$ and $\varsigma = 0.005$ are employed to obtain the results. The same value as the above damping ratio is employed for the standard damping ratio ς_{st} to calculate the localization strength κ. As can be observed in the figure, once ω_2 is given, one can maximize the localization strength by changing the coupling stiffness β. In other words, there exists a certain relation between ω_2 and β that can maximize the localization strength.

From now on, the effects of statistical properties of dimensionless parameters ω_i, β and ς on the frequency response localization will be discussed. The standard damping ratio $\varsigma_{st} = 0.005$ is employed to calculate κ throughout this study. First, the convergence of Monte Carlo simulation method is checked for typical cases. Table 1 shows typical convergence trends of the mean and the standard deviation of κ as well as probabilities

Table 1
Convergence of the statistical properties of the strength of frequency response localization versus number of samples in Monte Carlo simulation

Number of samples	Mean of κ		Standard deviation of κ		Probability of $\kappa \geqslant \kappa_c$	
	Tuned	Mistuned	Tuned	Mistuned	Tuned	Mistuned
10	1.115	1.198	0.041	0.064	0.600	0.700
100	1.100	1.178	0.058	0.072	0.530	0.390
1000	1.103	1.180	0.064	0.072	0.506	0.397
10000	1.102	1.181	0.066	0.074	0.501	0.405
100000	1.103	1.181	0.066	0.074	0.507	0.404

Tuned: $E(\omega_1) = 1.0$, $E(\omega_2) = 1.0$, $\sigma_{\omega_i} = 0.01$, $E(\beta) = 0.002$, $\bar{\sigma}_\beta = 0.05$, $E(\varsigma) = 0.005$, $\bar{\sigma}_\varsigma = 0.05$, $\kappa_c = 1.1$.
Mistuned: $E(\omega_1) = 1.0$, $E(\omega_2) = 1.024$, $\sigma_{\omega_i} = 0.01$, $E(\beta) = 0.012$, $\bar{\sigma}_\beta = 0.05$, $E(\varsigma) = 0.005$, $\bar{\sigma}_\varsigma = 0.05$, $\kappa_c = 1.2$.

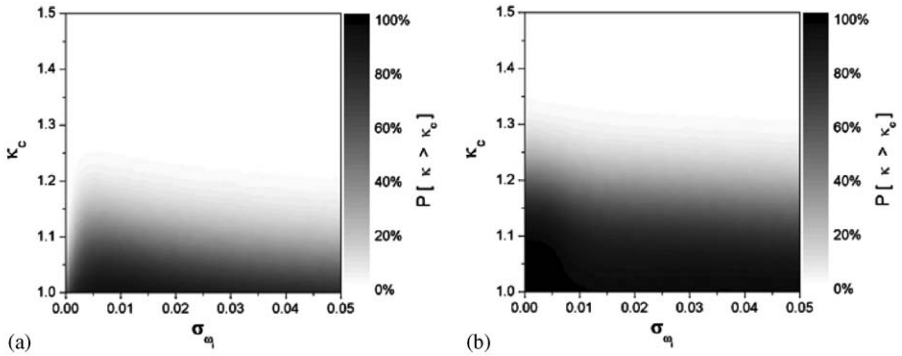

Fig. 4. Probability $\kappa \geqslant \kappa_c$ versus the standard deviation of ω_i's. (a) Tuned case ($E(\omega_1) = 1.0$, $E(\omega_2) = 1.0$, $E(\beta) = 0.002$, $E(\varsigma) = 0.005$, $\bar{\sigma}_\beta = 0.05$, $\bar{\sigma}_\varsigma = 0.05$), and (b) mistuned case ($E(\omega_1) = 1.0$, $E(\omega_2) = 1.024$, $E(\beta) = 0.012$, $E(\varsigma) = 0.005$, $\bar{\sigma}_\beta = 0.05$, $\bar{\sigma}_\varsigma = 0.05$).

of criteria (that κ exceeds certain values). Two cases of parameters are employed to obtain the results of the table, where the statistical properties of ω_i's, β and ς are given. The first case will be called hereafter the tuned case, where $E(\beta) = 0.002$, $\bar{\sigma}_\beta = 0.05$, $E(\varsigma) = 0.005$, $\bar{\sigma}_\varsigma = 0.05$, $E(\omega_1) = 1.0$, $E(\omega_2) = 1.0$ and $\sigma_{\omega_i} = 0.01$ are employed. The symbol $\bar{\sigma}_\beta$ denotes the normalized standard deviation of the coupling stiffness, i.e. $\sigma_\beta/E(\beta)$, and $\bar{\sigma}_\varsigma$ denotes the normalized standard deviation of the damping ratio, i.e. $\sigma_\varsigma/E(\varsigma)$. The second case will be called hereafter the mistuned case, where $E(\beta) = 0.012$, $\bar{\sigma}_\beta = 0.05$, $E(\varsigma) = 0.005$, $\bar{\sigma}_\varsigma = 0.05$, $E(\omega_1) = 1.0$, $E(\omega_2) = 1.024$ and $\sigma_{\omega_i} = 0.01$ are employed. The table shows that the statistical properties of the output converge reasonably fast as the number of sampling data increases. To save the computation time while maintaining reasonable simulation accuracy, 10,000 sampling data are employed to obtain the numerical results hereinafter.

Fig. 4 shows the probability of $\kappa \geqslant \kappa_c$ versus σ_{ω_i} (the standard deviation of ω_i's). All the statistical properties except σ_{ω_i} for the tuned and the mistuned cases are employed to obtain the results. It can be observed in Fig. 4(a) that the localization strength κ cannot exceed 1.25 for the tuned case. It can also be observed that the probability becomes relatively high at certain standard deviation range (around $\sigma_{\omega_i} = 0.005$ in this case). To reduce the probability of $\kappa \geqslant 1.1$ for this tuned system, one should avoid the region. In other words, if not reduced sufficiently, the reduction of σ_{ω_i} may increase the probability. Fig. 4(b) shows that the strength of localization can reach 1.35 for the mistuned case. However, as κ_c exceeds 1.2, the probability decreases rapidly. This figure also shows that the standard deviation of ω_i's does not significantly affect the probability for the mistuned system.

Fig. 5 shows the probability of $\kappa \geqslant \kappa_c$ in the plane of $\sigma_{\omega_2} - \sigma_{\omega_1}$. Again, all the statistical properties except σ_{ω_i} for the tuned and the mistuned cases are employed to obtain the results. A relatively high probability region (a quarter circle band) can be observed in Fig. 5(a). This indicates that one should reduce the square root sum of the standard deviations sufficiently if a very low probability is required. As discussed previously in Fig. 4(a),

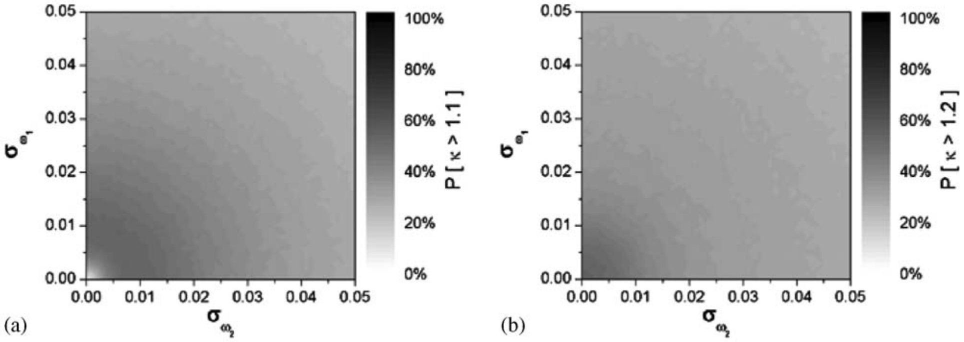

Fig. 5. Probability of $\kappa \geqslant \kappa_c$ in the plane of $\sigma_{\omega_2} - \sigma_{\omega_1}$. (a) Tuned case ($E(\omega_1) = 1.0$, $E(\omega_2) = 1.0$, $E(\beta) = 0.002$, $E(\varsigma) = 0.005$, $\bar{\sigma}_\beta = 0.05$, $\bar{\sigma}_\varsigma = 0.05$), and (b) mistuned case ($E(\omega_1) = 1.0$, $E(\omega_2) = 1.024$, $E(\beta) = 0.012$, $E(\varsigma) = 0.005$, $\bar{\sigma}_\beta = 0.05$, $\bar{\sigma}_\varsigma = 0.05$).

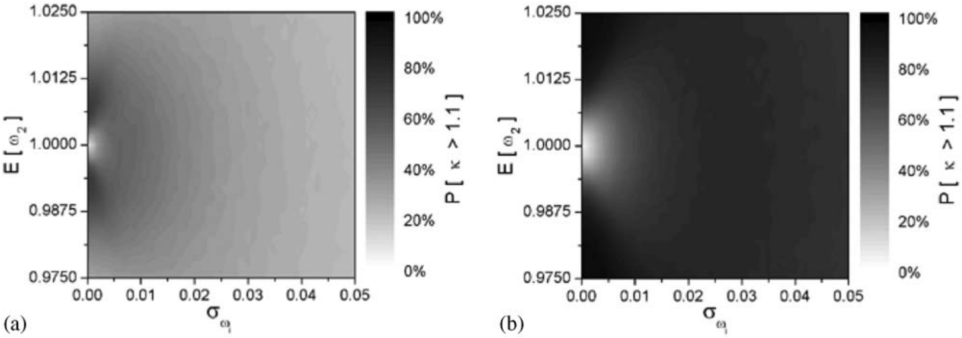

Fig. 6. Probability of $\kappa \geqslant 1.1$ in the plane of $\sigma_{\omega_i} - E[\omega_2]$. (a) Weaker coupling case ($E(\omega_1) = 1.0$, $E(\beta) = 0.002$, $E(\varsigma) = 0.005$, $\bar{\sigma}_\beta = 0.05$, $\bar{\sigma}_\varsigma = 0.05$), and (b) stronger coupling case ($E(\omega_1) = 1.0$, $E(\beta) = 0.012$, $E(\varsigma) = 0.005$, $\bar{\sigma}_\beta = 0.05$, $\bar{\sigma}_\varsigma = 0.05$).

a tactless reduction of σ_{ω_i} may increase the probability. Fig. 5(b) shows the results of the mistuned case. As shown in the figure, a relatively high probability region is concentrated around the origin. Since this system is intentionally designed to achieve certain strength of response localization, one might want to increase the probability as high as possible. As shown in the figure, the tolerance should be reduced sufficiently to achieve such target. However, even if the square root sum is decreased, the probability cannot exceed certain value with the criterion $\kappa \geqslant 1.2$. If the criterion were $\kappa \geqslant 1.1$, high probability could have been achieved even with relatively large σ_{ω_i}'s (see Fig. 4(b)).

Fig. 6 shows the probability of $\kappa \geqslant 1.1$ in the plane of $\sigma_{\omega_i} - E[\omega_2]$. All the statistical properties except σ_{ω_i} and $E(\omega_2)$ for the tuned and the mistuned cases are employed to obtain the results. One can observe that the probability of $\kappa \geqslant 1.1$ is increased with the stronger coupling stiffness value in most of the plane. However, as can be observed by comparing Figs. 6(a) and (b), the low-probability region (that exists around $E(\omega_2) = 1.0$ and $\sigma_{\omega_i} = 0$) is also significantly enlarged by the stronger coupling stiffness. Therefore, if the probability of certain strength response localization needs to be reduced, the mean value of the coupling stiffness needs to be increased while maintaining σ_{ω_i} within a certain small value range.

Fig. 7 shows the probability of $\kappa \geqslant \kappa_c$ in the plane of $\sigma_{\omega_i} - E[\beta]$. All the statistical properties except σ_{ω_i} and $E(\beta)$ for the tuned and the mistuned cases are employed to obtain the results. As can be observed from Fig. 7(a), there exists an approximate relation between $E(\beta)$ and σ_{ω_i} that maximize the probability (see the white broken solid line in Fig. 7(a)). The low probability can be achieved by staying away from the white broken solid line. If a certain small value for σ_{ω_i} is already given, it is more effective to increase $E(\beta)$ to reduce the probability as discussed in the previous paragraph. However, if the value for σ_{ω_i} is relatively large, it is more effective to decrease $E(\beta)$ to reduce the probability. For the mistuned case (shown in Fig. 7(b)),

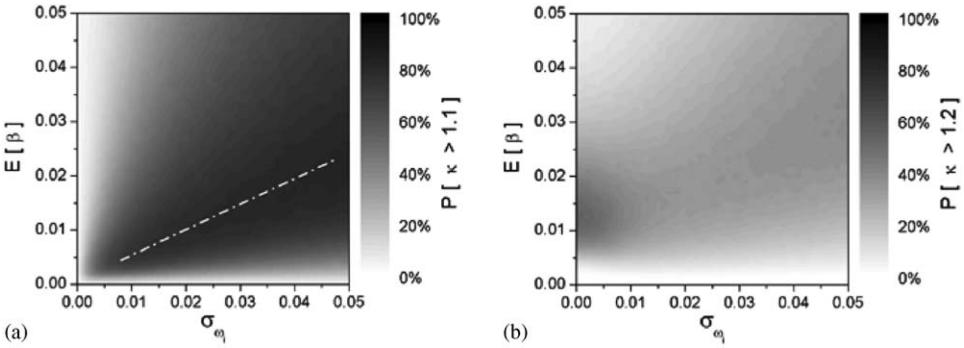

Fig. 7. Probability of $\kappa \geqslant \kappa_c$ in the plane of $\sigma_{\omega_i} - E[\beta]$. (a) Tuned case ($E(\omega_1) = 1.0$, $E(\omega_2) = 1.0$, $E(\varsigma) = 0.005$, $\bar{\sigma}_\beta = 0.05$, $\bar{\sigma}_\varsigma = 0.05$), and (b) mistuned case ($E(\omega_1) = 1.0$, $E(\omega_2) = 1.024$, $E(\varsigma) = 0.005$, $\bar{\sigma}_\beta = 0.05$, $\bar{\sigma}_\varsigma = 0.05$).

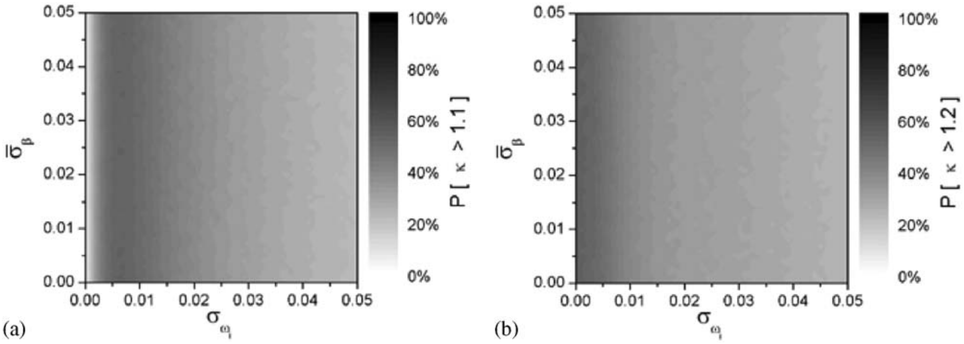

Fig. 8. Probability of $\kappa \geqslant \kappa_c$ in the plane of $\sigma_{\omega_i} - \bar{\sigma}_\beta$. (a) Tuned case ($E(\omega_1) = 1.0$, $E(\omega_2) = 1.0$, $E(\beta) = 0.002$, $E(\varsigma) = 0.005$, $\bar{\sigma}_\varsigma = 0.05$), and (b) mistuned case ($E(\omega_1) = 1.0$, $E(\omega_2) = 1.024$, $E(\beta) = 0.012$, $E(\varsigma) = 0.005$, $\bar{\sigma}_\varsigma = 0.05$).

providing a small value for σ_{ω_i} (less than 0.005) while maintaining $E(\beta)$ within the range of 0.01–0.015 is the most effective way to increase the probability.

Fig. 8 shows the probability of $\kappa \geqslant \kappa_c$ in the plane of $\sigma_{\omega_i} - \bar{\sigma}_\beta$. All the statistical properties except σ_{ω_i} and $\bar{\sigma}_\beta$ for the tuned and the mistuned cases are employed to obtain the results. To prevent negative coupling stiffness from being created by the random number generator, a restricted range of $\bar{\sigma}_\beta$ is considered here. The results of the figures show that the probability is rarely influenced by the standard deviation of the coupling stiffness in both cases. In other words, one need not prescribe a tight coupling stiffness tolerance to reduce (or enhance) the localization phenomena.

Fig. 9 shows the probability of $\kappa \geqslant \kappa_c$ in the plane of $\sigma_{\omega_i} - \bar{\sigma}_\varsigma$. All the statistical properties except σ_{ω_i} and $\bar{\sigma}_\varsigma$ for the tuned and the mistuned cases are employed to obtain the results. Fig. 9(a) shows that $\bar{\sigma}_\varsigma$ influences the probability slightly. However, if a very low probability is required, $\bar{\sigma}_\varsigma$ should be sufficiently decreased. Fig. 9(b) shows that $\bar{\sigma}_\varsigma$ as well as σ_{ω_i} needs to be decreased sufficiently to guarantee a very high localization probability for the mistuned case. Therefore, $\bar{\sigma}_\varsigma$ needs to be controlled tightly when a very low or high probability is required.

Fig. 10 shows the probability of $\kappa \geqslant \kappa_c$ in the plane of $\sigma_{\omega_i} - E[\varsigma]$. All the statistical properties except σ_{ω_i}, $E[\varsigma]$ and σ_ς for the tuned and the mistuned cases are employed to obtain the results. Instead of using $\bar{\sigma}_\varsigma = 0.05$ (which results in the variation of σ_ς as $E[\varsigma]$ varies), $\sigma_\varsigma = 0.0005$ is employed for the results of Fig. 10. As shown in the figures, the mean value of damping ratio $E[\varsigma]$ is the most critical factor for the localization strength. The probability can be easily decreased or increased by increasing or decreasing the mean value of the damping ratio in both cases. Therefore, even if the relative difference between two frequency response curves is significant (so that the responses are localized), the absolute value of the difference becomes small as $E[\varsigma]$ increases. One should note that $\varsigma_{st} = 0.005$ is employed in the present study.

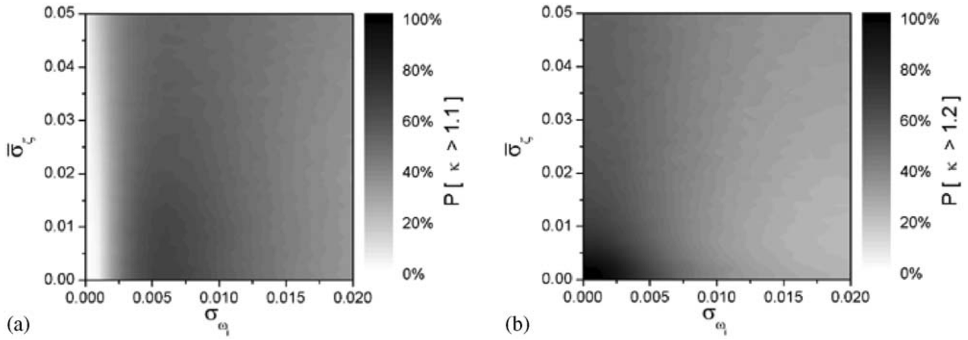

Fig. 9. Probability of $\kappa \geqslant \kappa_c$ in the plane of $\sigma_{\omega_i} - \bar{\sigma}_\varsigma$. (a) Tuned case ($E(\omega_1) = 1.0$, $E(\omega_2) = 1.0$, $E(\beta) = 0.002$, $E(\varsigma) = 0.005$, $\bar{\sigma}_\beta = 0.05$), and (b) mistuned case ($E(\omega_1) = 1.0$, $E(\omega_2) = 1.024$, $E(\beta) = 0.012$, $E(\varsigma) = 0.005$, $\bar{\sigma}_\beta = 0.05$).

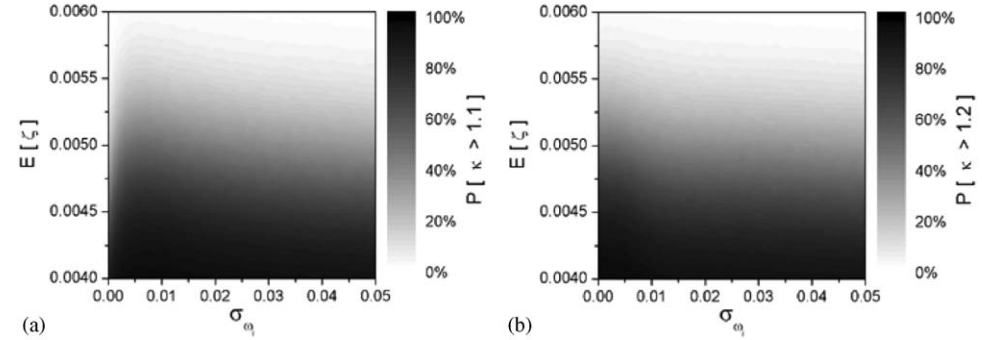

Fig. 10. Probability of $\kappa \geqslant \kappa_c$ in the plane of $\sigma_{\omega_i} - E[\varsigma]$. (a) Tuned case ($E(\omega_1) = 1.0$, $E(\omega_2) = 1.0$, $E(\beta) = 0.002$, $\bar{\sigma}_\beta = 0.05$, $\sigma_\varsigma = 0.0005$), and (b) mistuned case ($E(\omega_1) = 1.0$, $E(\omega_2) = 1.024$, $E(\beta) = 0.012$, $\bar{\sigma}_\beta = 0.05$, $\sigma_\varsigma = 0.0005$).

It is difficult to investigate the frequency response localization properties of a nearly periodic system if too many statistical parameters are involved in the system. Therefore, only the double pendulum case has been considered so far. The statistical effects of the coupling parameter and the damping parameter on the frequency localization properties are clearly exhibited with the simple model. Such effects are true for multi-degree models, too. In the following, effects of some statistical parameter properties along with the number of subcomponents on the probability of frequency response localization will be discussed.

In Fig. 11, variations of the probability versus the standard deviation of ω_i's for various subcomponent numbers are given. All the statistical properties except σ_{ω_i} for the tuned case are employed to obtain the results. As can be shown in the figure, the probability increases as the number of subcomponents increases. It can also be observed that the standard deviation where the maximum probability occurs decreases as the number of subcomponents increases. Thus, to reduce the probability sufficiently, the standard deviation σ_{ω_i} should be decreased more as the number of subcomponents increases. Therefore, in general, it becomes more difficult to achieve a low-probability design as the number of subcomponents increases.

In Fig. 12, variations of the probability versus the mean value of β for various subcomponent numbers are given. All the statistical properties except $E(\beta)$ for the tuned case are employed to obtain the results. For a periodic system having small number of subcomponents, a low-probability design can be achieved by increasing $E(\beta)$. However, as the number of subcomponents increases, the probability is only slightly influenced by $E(\beta)$ in its large value range. Also, the value of $E(\beta)$ where the maximum probability occurs increases as the number of subcomponents increases. Therefore, for periodic systems having large number of subcomponents, it is more effective to choose a small value for $E(\beta)$ to achieve a low-probability design.

In Fig. 13, variations of the probability versus the normalized standard deviation of β for various subcomponent numbers are given. All the statistical properties except $\bar{\sigma}_\beta$ for the tuned case are employed to obtain the results. As can be shown in the figure, the probability is rarely influenced by $\bar{\sigma}_\beta$ (even if it increases

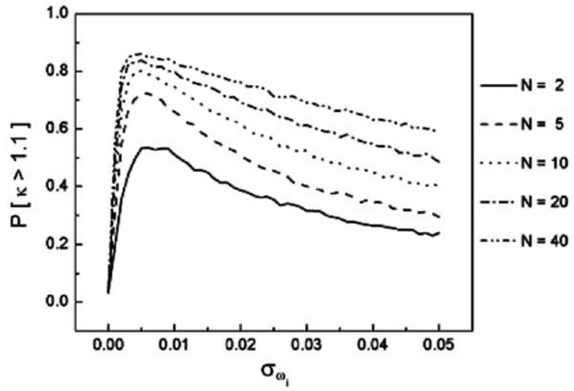

Fig. 11. Probability variations versus σ_{ω_i} for various subcomponent numbers ($E(\omega_i) = 1.0$, $E(\beta) = 0.002$, $E(\varsigma) = 0.005$, $\bar{\sigma}_\beta = 0.05$, $\bar{\sigma}_\varsigma = 0.05$).

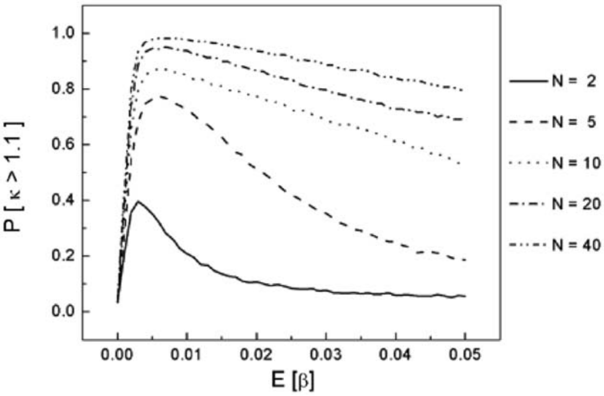

Fig. 12. Probability variations versus $E(\beta)$ for various subcomponent numbers ($E(\omega_i) = 1.0$, $E(\varsigma) = 0.005$, $\sigma_{\omega_i} = 0.002$, $\bar{\sigma}_\beta = 0.05$, $\bar{\sigma}_\varsigma = 0.05$).

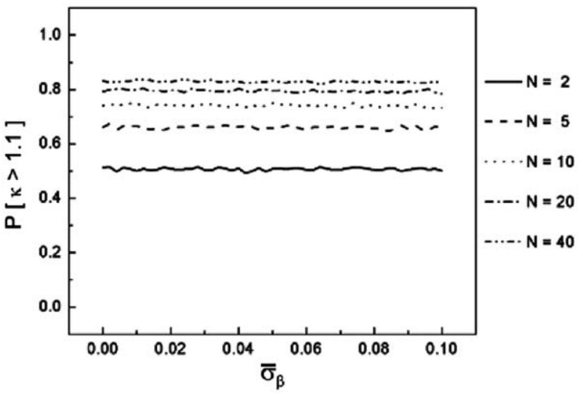

Fig. 13. Probability variations versus $\bar{\sigma}_\beta$ for various subcomponent numbers ($E(\omega_i) = 1.0$, $E(\beta) = 0.002$, $E(\varsigma) = 0.005$, $\sigma_{\omega_i} = 0.01$, $\bar{\sigma}_\varsigma = 0.05$).

as the number of subcomponents increases). Therefore, $\bar{\sigma}_\beta$ is not a good factor to control the frequency response localization.

In Fig. 14, variations of the probability versus the mean of ς for various subcomponent numbers are given. All the statistical properties except $E(\varsigma)$ for the tuned case are employed to obtain the results. As the mean of ς

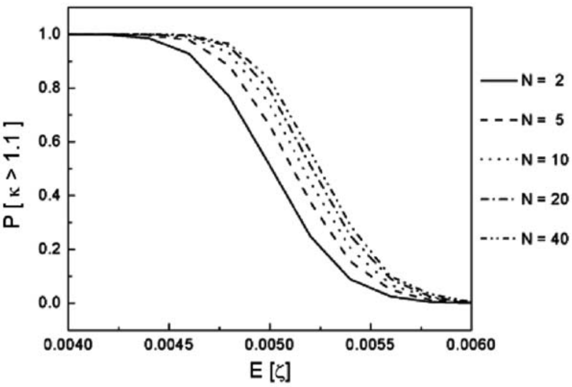

Fig. 14. Probability variations versus $E(\varsigma)$ for various subcomponent numbers ($E(\omega_i) = 1.0$, $E(\beta) = 0.002$, $\sigma_{\omega_i} = 0.01$, $\bar{\sigma}_\beta = 0.05$, $\bar{\sigma}_\varsigma = 0.05$).

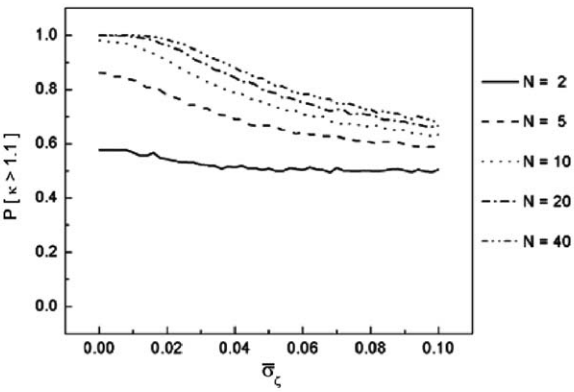

Fig. 15. Probability variations versus $\bar{\sigma}_\varsigma$ for various subcomponent numbers ($E(\omega_i) = 1.0$, $E(\beta) = 0.002$, $E(\varsigma) = 0.005$, $\sigma_{\omega_i} = 0.01$, $\bar{\sigma}_\beta = 0.05$).

increases, the probability decreases rapidly. With fixed value of $E(\varsigma)$, the probability increases asymptotically as the number of subcomponents increases.

In Fig. 15, variations of the probability versus the normalized standard deviation of ς for various subcomponent numbers are given. All the statistical properties except $\bar{\sigma}_\varsigma$ for the tuned case are employed to obtain the results. As can be shown in the figure, the probability is rarely influenced by $\bar{\sigma}_\varsigma$ when the number of subcomponents is small. But as the number of subcomponents increases, the probability decreases slightly as $\bar{\sigma}_\varsigma$ increases.

4. Conclusions

In the present study, the effects of statistical properties of the natural frequency, the coupling stiffness and the damping ratio of a periodic system on the strength of frequency response localization are investigated through Monte Carlo simulation. The strength of frequency response localization is defined and the probabilities that the localization strength exceeds certain values are calculated. It is found that the probabilities are significantly influenced by some statistical properties of parameters. Especially, σ_{ω_i}'s, $E(\beta)$, and $E[\varsigma]$ turn out to be the most sensitive factors for the frequency response localization. As the number of subcomponents of a periodic system increases, the localization strength asymptotically increases in general. It is also found that $E(\beta)$ needs to determined differently to control the statistical characteristics of frequency response localization as the number of subcomponents increases.

Acknowledgments

This research was supported by Innovative Design Optimization Technology Engineering Research Center through research fund, for which the authors are grateful.

References

[1] P.W. Anderson, Absence of diffusion in certain random lattices, *Physical Review* 109 (5) (1958) 1492–1505.
[2] D.J. Ewins, The effect of detuning upon the forced vibrations of bladed disks, *Journal of Sound and Vibration* 9 (1) (1969) 65–79.
[3] D.J. Ewins, A study of resonance coincidence in bladed disks, *Journal of Mechanical Engineering Science* 12 (1970) 305–312.
[4] D.J. Ewins, Vibration characteristics of bladed disc assemblies, *Journal of Mechanical Engineering Science* 15 (3) (1973) 165–186.
[5] D.J. Ewins, Vibration modes of mistuned bladed disks, *ASME Journal of Engineering for Power* (1976) 349–355.
[6] O.O. Bendiksen, Flutter of mistuned turbomachinery rotors, *Journal of Engineering for Gas Turbines and Power* 106 (1) (1984) 25–33.
[7] O.O. Bendiksen, Mode localization phenomena in large space structure, *AIAA Journal* 25 (9) (1987) 1241–1248.
[8] C. Pierre, D.M. Tang, E.H. Dowell, Localized vibrations of disordered multispan beams: theory and experiment, *AIAA Journal* 25 (9) (1987) 1249–1257.
[9] C. Pierre, E.H. Dowell, Localization of vibration by structural irregularity, *Journal of Sound and Vibration* 114 (3) (1987) 549–564.
[10] S.T. Wei, C. Pierre, Localization phenomena in mistuned assemblies with cyclic symmetry [Part I] free vibrations, [Part II] forced vibrations, *Journal of Vibration, Acoustics, Stress, and Reliability in Design* 110 (1988) 429–449.
[11] P. Castanier, C. Pierre, Consideration on the benefits of intentional blade mistuning for the forced response of turbomachinery rotors, *Analysis and Design Issues for Modern Aerospace Vehicles* 55 (1997) 419–425.
[12] C.H. Hodges, J. Woodhouse, Vibration isolation form irregularity in a nearly periodic structure: theory and measurements, *Journal of the Acoustical Society of America* 74 (3) (1983) 894–905.
[13] C. Pierre, Weak and strong vibration localization in disordered structures: a statistical investigation, *Journal of Sound and Vibration* 139 (1) (1990) 111–132.
[14] G.Q. Cai, Y.K. Lin, Statistical distribution of frequency response in disordered periodic structures, *AIAA Journal* 30 (5) (1992) 1400–1407.
[15] R.S. Langley, The statistics of wave transmission through disordered periodic waveguides, *Journal of Sound and Vibration* 189 (4) (1996) 421–441.
[16] H.H. Yoo, J.Y. Kim, D.J. Inman, Vibration localization of simplified mistuned cyclic structures undertaking external harmonic force, *Journal of Sound and Vibration* 261 (5) (2003) 859–870.
[17] W.H. Huang, Vibration of some structures with periodic random parameters, *AIAA Journal* 20 (7) (1982) 1001–1008.
[18] A. Sinha, Calculating the statistics of forced response of a mistuned bladed disk assembly, *AIAA Journal* 24 (11) (1986) 1797–1801.
[19] S.T. Wei, C. Pierre, Statistical analysis of the forced response of mistuned cyclic assemblies, *AIAA Journal* 28 (5) (1990) 861–868.